Terahertz Magnetoelectric Resonance Enhanced by Mutual Coupling of Electromagnons

Y. Takahashi,[1] Y. Yamasaki,[2] and Y. Tokura[1,3]

[1]*Department of Applied Physics and Quantum Phase Electronics Center (QPEC), University of Tokyo, Tokyo 113-8656, Japan*
[2]*Photon Factory and Condensed Matter Research Center, Institute of Materials Structure Science, High Energy Accelerator Research Organization, Tsukuba, Ibaraki 305-0801, Japan*
[3]*RIKEN Center for Emergent Matter Science (CEMS), Wako, 351-0198, Japan*

(Received 30 March 2013; published 17 July 2013)

Both electric- and magnetic-dipole active spin excitations, i.e., electromagnons, which mediate the dynamical magnetoelectric effect, have been investigated for a multiferroic perovskite of manganite by optical spectroscopy at terahertz frequencies. Upon the magnetoelectric resonance at 1 meV in the multiferroic phase with the *bc*-plane spin cycloidal order, a gigantic dynamical magnetoelectric effect has been observed as a nonreciprocal directional dichroism or birefringence. The light *k*-vector-dependent difference ($\Delta\kappa = \kappa_+ - \kappa_-$) of the extinction coefficient ($\kappa_\pm$) is as large as $\Delta\kappa \sim 1$ or $2\Delta\kappa/(\kappa_+ + \kappa_-) \sim 0.7$ at the lowest-lying electromagnon energy. We clarified the mutual coupling of the $E^\omega \parallel a$-polarized electromagnons of the different origins, leading to the enhancement of the magnetoelectric resonance.

DOI: 10.1103/PhysRevLett.111.037204 PACS numbers: 75.80.+q, 75.40.Gb, 75.85.+t, 76.50.+g

The magnetoelectric effect (ME) has been attracting attention in the past decade due to the discovery of intrinsic multiferroics [1], in which the particular spin order is responsible for the presence of the ferroelectric order [2–5]. One unique mechanism combining ferroelectricity and spin order is effective in the cycloidal spin order as described by the spin-current (SC) model [6] or the inverse Dzyaloshinskii-Moriya interaction [7]. In this model, the local electric polarization is proportional to $e_{ij} \times (S_i \times S_j)$; here, e_{ij} is a unit vector connecting the adjacent spins S_i and S_j. The cycloidal spin structure leads to the net polarization lying in the cycloidal spin plane and perpendicular to e_{ij} [see Fig. 1(a)].

One of the intriguing aspects of multiferroics is a unique dynamical magnetoelectric effect mediated by their elementary excitations. The spin excitation endowed with electric activity, referred to as "electromagnon," has been discovered in the representative multiferroic perovskite $R\mathrm{MnO_3}$ (where R is rare earth) as optical absorption in a terahertz region [8]. The SC mechanism can activate the electromagnon as well as the ferroelectric polarization (P); the rotational vibration mode of the cycloidal spin plane around the magnetic modulation vector q_m accompanies a fluctuation of P as shown in Fig. 1(a), and is hence electric-dipole active [9,10]. Thus this electromagnon excitation is allowed when the polarization of light is perpendicular to the P, for instance $E^\omega \parallel a$ for $P \parallel c$ in the *bc*-plane cycloidal spin state [see Fig. 1(a) and mode I in 1(c)] or $E^\omega \parallel c$ for $P \parallel a$ in the *ab*-plane cycloidal spin state. On the other hand, the exchange-striction mechanism can also generate the electromagnon excitation, in which the embedded local electric dipole moment between the spin sites gives rise to the spin waves for the noncollinear spin states [8,11]. This exchange-striction mechanism derives two broad absorption peaks in the cycloidal spin phases, while the polarization selection rule ($E^\omega \parallel a$) for these electromagnons is irrespective of the P direction or of the cycloidal spin plane (*ab* or *bc* plane). Among the two exchange-striction induced modes, the higher lying one has been assigned to the zone-edge mode of the spin wave ($q = \pi$; 9 meV for $R = \mathrm{Gd_{0.5}Tb_{0.5}}$ [12]). The lower-lying mode is assigned to the spin wave with $q = \pi - 2q_m$ [Fig. 1(b) and mode II in 1(c)], as electrically activated by the additional contribution from the magnetic anisotropy [13].

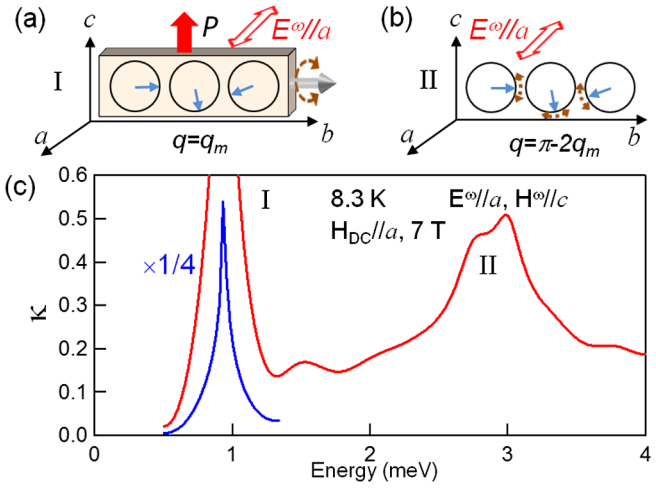

FIG. 1 (color online). (a) Schematics of the *bc*-plane cycloidal spin state and ferroelectric polarization (P). Mode I (spin-current (SC)-driven electromagnon); rotational vibration of the cycloidal spin plane around the *b*-axis ($q = q_m$) is driven by the light polarization of $E^\omega \parallel a$. (b) Mode II (exchange-striction induced electromagnon); rotational vibration of spins around the *a*-axis ($q = \pi - 2q_m$) is driven by the light polarization of $E^\omega \parallel a$. (c) Imaginary part κ of refractive index for ($E^\omega \parallel a$, $H^\omega \parallel c$) at 8.3 K under the magnetic field along the *a*-axis (7 T).

A remarkable property of SC-driven electromagnons is their inherent ME coupling between the induced polarization P^ω and magnetization M^ω, resulting in the optical (dynamical) magnetoelectric (OME) effect allowed by the simultaneous breaking of time-reversal and space-inversion symmetry, i.e., the presence of P and magnetization (M) [10,14]. The OME effect can be observed as the nonreciprocal directional dichroism for the linearly polarized light; a matter shows different optical responses to the oppositely propagating light [15,16]. Thus the OME effect is distinguished from the conventional magneto-optical (Faraday and Cotton-Mouton) effects. By contrast, the lack of such a cross coupling was anticipated for the electromagnon modes driven by the exchange-striction mechanism, since these electromagnon modes are not magnetic-dipole active due to their $q \neq 0$ nor $q \neq q_m$ nature [10]. In this Letter, we report on the gigantic OME effect due to the SC-driven electromagnon resonance enhanced via coupling with the higher-lying exchange-striction driven electromagnon modes in the bc-plane cycloidal spin state of $Gd_{0.5}Tb_{0.5}MnO_3$ [17]. The enhanced magnitude of the resonant OME effect is 20 times as large as that for the ab-plane cycloidal spin state, where the coupling between the SC- and exchange-striction driven electromagnon modes is prohibited.

A single crystal of $Gd_{0.5}Tb_{0.5}MnO_3$ was synthesized by a floating zone method. The ac-plane sample with specular surface with the thickness of 500 μm and 3.5 mm in the diameter was prepared for terahertz transmittance measurements. To measure the optical constant from 0.5 to 4 meV, a time-domain terahertz spectroscopy was employed [10]. An external magnetic field was applied up to 7 T, perpendicular to the light propagation vector (in a Voigt configuration). To make an electrical contact to the sample, we put the silver paste on the both sides (c-planes), which were connected to the coaxial cables. In the cooling process, both magnetic (7 T, $H_{DC} \parallel a$) and electric (>1 kV/cm, $E_{DC} \parallel c$) fields were applied, and the single ME domain was formed by this ME cooling procedure [18].

Figure 1(c) shows the imaginary part κ of the refractive index of light polarization ($E^\omega \parallel a$, $H^\omega \parallel c$) for the bc-plane cycloidal spin state ($P \parallel c$). In this phase, the SC-driven electromagnon appears for $E^\omega \parallel a$, as well as the exchange-striction induced electromagnon which is always active for $E^\omega \parallel a$. In fact, two peaks are observed at 1 meV and 3 meV, corresponding to these electromagnons. Higher-lying peak at 3 meV has been assigned to the electromagnon induced by exchange-striction with $q = \pi - 2q_m$ (mode II) [12,13]. Lower-lying resonance at 1 meV, which shows a relatively sharp peak structure and larger peak intensity, can be attributed to the SC-driven electromagnon. Resonance energy is similar to that observed previously for the $E^\omega \parallel c$ SC-driven electromagnon mode in the ab-plane cycloidal state (0.8 meV), while the peak intensity is more than 40 times larger [10].

We can confirm this assignment by examining the cross-coupling nature of the SC-driven electromagnons, that manifests itself as the directional dichroism or birefringence. The first-order dynamical ME effect, which contributes to the linear optical response, can be described by the dynamical ME tensor $\alpha_{ij}(\omega)$ in addition to the conventional dynamical dielectric [$\chi^{ee}(\omega)$] and magnetic susceptibility [$\chi^{mm}(\omega)$],

$$\begin{aligned} P_i^\omega &= \chi_{ii}^{ee}(\omega)E_i^\omega + \alpha_{ij}(\omega)H_j^\omega \\ M_j^\omega &= \chi_{jj}^{mm}(\omega)H_j^\omega + \alpha_{ij}(\omega)E_i^\omega. \end{aligned} \tag{1}$$

The presence of the finite $\alpha_{ij}(\omega)$ is allowed by the simultaneous breaking of time-reversal and space-inversion symmetry. As illustrated in Fig. 2(a), the presence of orthogonal P and M ensures the finite $\alpha_{ij}(\omega)$ for the light propagating parallel to the vector product of them ($P \times M$), leading to the non-reciprocal directional dichroism for linear polarized-light. By combining above equations with Maxwell's equations, the directional complex refractive index for the light with $\pm k^\omega$ can be described as follows [19]:

$$N_\pm(\omega) = n(\omega) + i\kappa(\omega) = [n_0(\omega) + i\kappa_0(\omega)] \pm \alpha_{ij}(\omega). \tag{2}$$

In addition to the ordinary term of the refractive index $[n_0(\omega) + i\kappa_0(\omega)]$, the real and imaginary parts of $\alpha_{ij}(\omega)$ contribute to the optical response to induce the directional birefringence and dichroism. The reversal of either one of three vector parameters (P, M and k^ω) results in a sign change of $\alpha_{ij}(\omega)$ in the refractive index $N_\pm(\omega)$. Since the bc-plane cycloidal spin state ($P \parallel c$) gives no net magnetization, the magnetic field along the a-axis was applied to induce the $M \parallel a$ to produce the transverse conical spin state while keeping the $P(\parallel c)$ almost intact [see Fig. 2(a)]. The polarized light ($E^\omega \parallel a$, $H^\omega \parallel c$) with $k^\omega \parallel b$ can probe the OME effect on the electromagnon. In our experiment, the optical response in the four possible configurations defined by combination of $\pm P$ and $\pm M$ with a fixed k^ω, which can be grouped into two equivalent states in terms of the sign of $P \times M$ [Fig. 2(b)], were examined. For example, an optical response measured for ($P \parallel +c$, $M \parallel +a$) configuration provides spectra indicated by ($+P$, $+M$) in Fig. 2(c).

As shown in Fig. 2(c), the resonance of SC-driven electromagnon at 1 meV exhibits remarkable differences in line with the sign of the OME effect ($P \times M$), providing a compelling evidence for occurrence of the OME effect and also justifying our assignment. The OME spectra can be evaluated by the difference between N_+ and N_- for the four possible combinations of ($\pm P$, $\pm M$) [Fig. 2(d)]; for instance, the spectra for ($+P$, $+M$) and ($+P$, $-M$), which are categorized into the different states (N_- and N_+) by the sign of $P \times M$, give the OME spectra indicated by ($+P$, $-M$)-($+P$, $+M$). The sharp resonance peak in

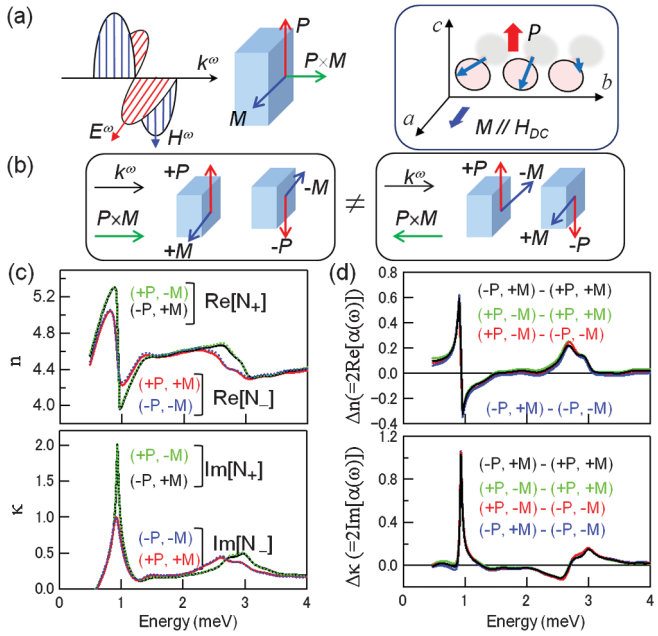

FIG. 2 (color). (a) Experimental configuration for the observation of the OME effect. Under a magnetic field along the a-axis, the bc-plane cycloidal spin state induces the cross-coupled $P(\| c)$ and $M(\| a)$. The polarized light with ($E^\omega \| a$, $H^\omega \| c$) fulfills the condition of the OME effect [$k^\omega \| (P \times M)$], and excites the both electromagnon modes (modes I and II). (b) Configurations of P, M and k^ω, and their relations for the observation of the OME effect (see text). (c) Complex refractive indices, n and κ, in the different conditions for OME observation at 8.3 K and 7 T. (d) Difference (Δn and $\Delta\kappa$) spectra derived from (c). Results for four possible combinations to obtain $\Delta\kappa$ are shown. The respective four curves indistinguishably overlap with each other, as expected.

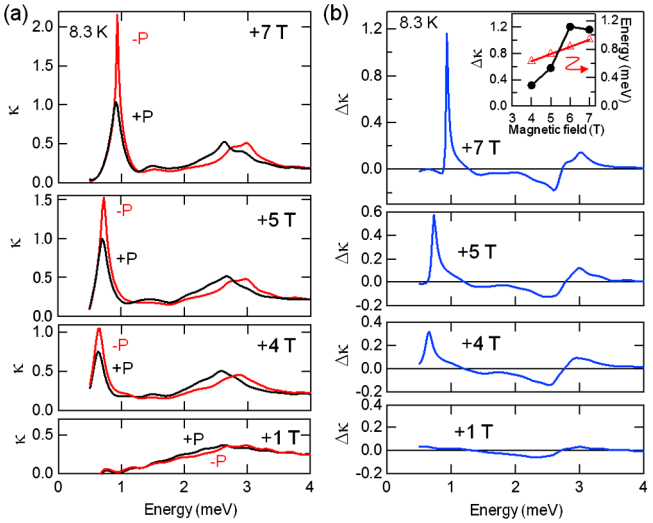

FIG. 3 (color online). (a) Magnetic field ($H_{DC} \| a$) dependence of imaginary part κ of the refractive index at 8.3 K. (b) Difference spectra of κ derived from (a). Inset: Magnetic field dependence of peak energies and peak intensities of $\Delta\kappa$ for the SC-driven electromagnon (mode I).

$\Delta\kappa$ as well as the clear dispersive structure in Δn around 1 meV manifests the large ME resonance with the SC-driven electromagnon. Their magnitudes exceed 1 in the complex refractive index. Around the peak of the exchange-striction induced electromagnon, a broad ME signal is discernible from 2 to 4 meV, indicating the presence of converse cross-coupling effect also in this electromagnon mode.

Figure 3 shows the magnetic field dependence of (a) spectra of the imaginary part κ of the refractive index and (b) OME spectra represented by $\Delta\kappa$. The resonance energy of SC-driven electromagnon is governed by the anisotropy between the ab-plane and bc-plane cycloidal states as well as the external magnetic field [9]. Since an applied magnetic field along the a axis stabilizes the bc-plane cycloidal state, the SC-driven electromagnon peak shifts to higher energy with increasing magnetic field [see inset to Fig. 3(b)]. A similar behavior has also been observed in the ab-plane cycloidal state when the magnetic field is applied along the c axis [10]. Directional dichroism should show the linear M dependence in the neighborhood of zero magnetization due to the first-order nature of ME effect. While an increase of peak intensity of $\Delta\kappa$ is observed up to 6 T [inset to Fig. 3(b)], it appears to be saturated around 7 T, indicating that the OME effect tends to be beyond the linear response regime.

These noticeable features, i.e., the intensified SC-driven electromagnon and the gigantic OME effects of the both electromagnons, suggest a mutual coupling of the electromagnons of different origins. For comparison, we can refer to the ab-plane cycloidal spin state ($P \| a$) in the series of $R\mathrm{MnO_3}$, in which the SC-driven electromagnon is decoupled from the exchange-striction induced electromagnons because of different polarization selection rules: The SC-driven electromagnon is active for $E^\omega \| c$ in the ab-plane cycloidal spin state ($P \| a$), whereas the exchange-striction driven electromagnon is always for $E^\omega \| a$. In Fig. 4, we summarized (a) spectral weights (SWs) of electromagnons, (b) SWs of OME, and (c) OME spectra for the bc-plane ($R = \mathrm{Gd_{0.5}Tb_{0.5}}$) and the ab-plane ($R = \mathrm{Eu_{0.55}Y_{0.45}}$) cycloidal spin states. (The latter data are extracted from Ref. [10]; see also Ref. [20].)

In order to deduce the bare SW of electromagnon in the presence of the OME effect, the ordinary term spectra of refractive indices, $n_0 + i\kappa_0 = [N_+(\omega) + N_-(\omega)]/2$, were used. Then, the spectra of the SC-driven electromagnon were fitted with Lorentz functions. The SW is defined by the effective number of electrons,

$$N_{\mathrm{eff}} = \frac{2m_0 V}{\pi e^2} \int_{0.5\ \mathrm{meV}}^{4\ \mathrm{meV}} \sigma(\omega')d\omega', \qquad (3)$$

where m_0 and V are the bare electron mass and the cell volume per Mn site, respectively. The magnetic field dependence of the SW of SC-driven electromagnon is plotted in Fig. 4(a). While comparable resonance energies for the

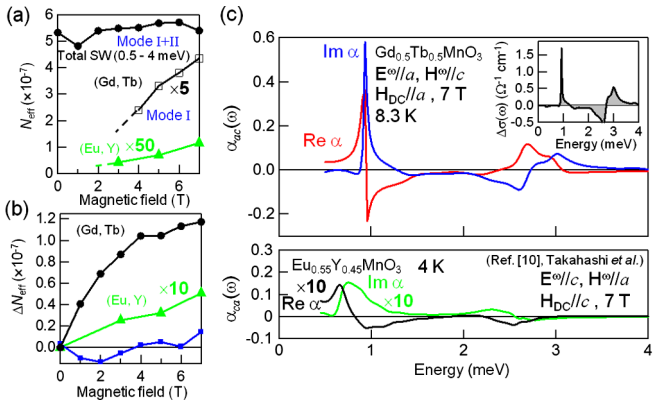

FIG. 4 (color online). (a) Magnetic field dependence of spectral weight (SW; see text for the definition) for the SC-driven electromagnon (mode I) for $R = Gd_{0.5}Tb_{0.5}$ (square) and $Eu_{0.55}Y_{0.45}$ (triangle). Total SW (ModeI + II) from 0.5 to 4 meV (circle) for $R = Gd_{0.5}Tb_{0.5}$ are also plotted. (b) Magnetic field dependence of the magnetoelectric (ME) spectral weight $\Delta N_{\rm eff}$ (see text for definition) for $R = Gd_{0.5}Tb_{0.5}$ (circles) and $Eu_{0.55}Y_{0.45}$ (triangles) are plotted. SW of $\Delta\sigma(\omega)$ (0.5 to 4 meV) for $R = Gd_{0.5}Tb_{0.5}$ is displayed by squares. (c) Complex ME spectra for the two materials. Inset shows the ME conductivity spectra.

ab-plane (0.8 meV) and the *bc*-plane (1 meV) cycloidal states are observed at 7 T for the SC-driven electromagnons, the latter state (squares) shows roughly 40 times larger SW than that in the former state (triangles). Since this electromagnon has its origin in the fluctuation of the magnetically-induced spontaneous P, the SW would be expected to be proportional to P^2 [9]. However, more than an order of magnitude larger SW for the *bc*-plane cycloidal state contradicts to the simple estimate based on the values of spontaneous P: 300 μC/m^2 for the *bc*-plane cycloid ($R = Gd_{0.5}Tb_{0.5}$) [17] and 900 μC/m^2 for the *ab*-plane cycloid ($R = Eu_{0.55}Y_{0.45}$) [10]. Thus the enhanced SW of SC-driven electromagnon in the *bc*-plane cycloidal state suggests a large amount of SW transfer from the exchange-striction induced ones.

The SW of the SC-driven electromagnon shows a steep increase with increasing magnetic field [open squares in Fig. 4(a)], while the total SW from 0.5 to 4 meV, including the both electromagnons I and II [(Fig. 1(c)], are almost conserved (circles). This result evidences that the SW transfer is allowed between the two electromagnons of different origins, resulting in their strong mutual coupling. The electric dipole activity may contribute to this mutual coupling of electromagnons.

Figure 4(c) shows the ME spectra; the ME tensor $\alpha_{ij}(\omega)$ is given by the relation, $\alpha_{ij}(\omega) = [N_+(\omega) - N_-(\omega)]/2$, from Eq. (2). ME tensor $\mathrm{Im}[\alpha_{ij}(\omega)]$ for the *bc*-plane cycloidal state (upper panel) shows 30 times larger peak intensity than that of the *ab*-plane one (lower panel) at the resonance of the SC-driven electromagnon. In addition to this pronounced resonance, a broad ME resonance is discerned around 3 meV, which corresponds to the peak of the electromagnon driven by the exchange-striction (mode II). The genuine exchange-striction-induced electromagnon would show no cross-coupling nature by itself as in the case of the *ab*-plane cycloidal state, but the coupling with the lower-lying SC-driven electromagnon gives rise to the noticeable OME effect in the present case of exchange-striction induced electromagnon.

To quantify the enhanced OME effect, we define the SW responsible for the OME effect as follows:

$$\Delta N_{\rm eff} = \frac{2m_0 V}{\pi e^2} \int_{0.5\ \mathrm{meV}}^{4\ \mathrm{meV}} |\Delta\sigma(\omega')| d\omega'. \qquad (4)$$

Here, the absolute value of ME optical conductivity $\Delta\sigma(\omega) = \sigma_+(\omega) - \sigma_-(\omega)$ [the shaded region in the inset to Fig. 4(c)] is integrated over the energy region of the two electromagnon modes, I and II; $\sigma_+(\omega)$ and $\sigma_-(\omega)$ correspond to the optical conductivity for $N_+(\omega)$ and $N_-(\omega)$, respectively. The $\Delta N_{\rm eff}$ values of the *bc* plane (circles) and the *ab* plane (triangles) cycloidal states both increase as the magnetic field is increased [Fig. 4(b)]. The observed $\Delta N_{\rm eff}$ for the *bc*-plane cycloidal state at 7 T is 20 times as large as the value for the *ab*-plane cycloidal state, confirming the enhancement of the OME effect through the coupling of electromagnons. We have also checked the sum rule that the integration of $\Delta\sigma(\omega)$ over all energy regions should equal zero. The sum of the OME SW ($2m_0V/\pi e^2 \int \Delta\sigma(\omega) d\omega$) from 0.5 to 4 meV [squares in Fig. 4(b)] is less than 15% of $\Delta N_{\rm eff}$ (circles) at 7 T, indicating that the SW transfer due to the OME effect is almost completed within the energy range of the two electromagnons (modes I and II).

The first observation of OME effect was reported as a relatively small directional birefringence ($\Delta n \sim 10^{-10}$) in molecular liquids [21]. Subsequent studies reported directional dichroism on several particular resonances; crystal-field transitions of *f*-electrons in visible regions [22] and of *d*-electrons in x ray [23], visible and near-infrared [24,25], and far-infrared regions [26], as well as the SC-driven electromagnon [10]. Although the OME effects have been identified in these studies, a magnitude of directional dichroism has been of the order of $\Delta\kappa \sim 10^{-2}$ at most. The present case exhibits remarkably large OME responses, in which $\Delta\kappa$ exceeds 1 or $\Delta\kappa/\kappa_0$ amounts to 0.7 at the resonance of the SC-driven electromagnon.

In conclusion, we have investigated the OME response of electromagnons for the *bc*-plane cycloidal spin state of $Gd_{0.5}Tb_{0.5}MnO_3$ by terahertz spectroscopy. The resonantly enhanced OME effects (directional dichroism) for the SC-driven electromagnon has been conclusively demonstrated in line with the sign of the OME effect, i.e., $P \times M$. The conspicuous spectral-weight transfer between electromagnons confirms their mutual strong coupling. By comparison with the *ab*-plane cycloidal spin state, in which these electromagnons are decoupled, the enhancement of the electromagnon resonance and the OME effect were estimated quantitatively. This colossal OME effect (Δn, $\Delta\kappa \sim 1$),

which enables additional control of the optical responses, will open a way to the new ME optics in a gigahertz-to-terahertz frequency region. Further enhancement of the OME effect based on this mechanism promises a negative refractive index as predicted under the presence of toroidal moment [27]. The control of P by the high field excitation of the electromagnon induced by the exchange-striction is predicted for $R\mathrm{MnO}_3$ [28]. Since this enhanced ME resonance is directly associated with the coupled fluctuation of P and M, optical high field excitation of this resonance will be more useful for the control of multiferroicity.

This work was partly supported by JSPS Grants-in-Aid for Scientific Research (No. 24840012 and No. 24224009) and the FIRST program by the Japan Society for the Promotion of Science.

[1] T. Kimura, T. Goto, H. Shintani, K. Ishizaka, T. Arima, and Y. Tokura, Nature (London) **426**, 55 (2003).
[2] W. Eerenstein, N. D. Mathur, and J. F. Scott, Nature (London) **442**, 759 (2006).
[3] S-W. Cheong and M. Mostovoy, Nat. Mater. **6**, 13 (2007).
[4] Y. Tokura and S. Seki, Adv. Mater. **22**, 1554 (2010).
[5] T. Arima, J. Phys. Soc. Jpn. **80**, 052001 (2011).
[6] H. Katsura, N. Nagaosa, and A. V. Balatsky, Phys. Rev. Lett. **95**, 057205 (2005).
[7] M. Mostovoy, Phys. Rev. Lett. **96**, 067601 (2006).
[8] A. Pimenov, A. A. Mukhin, V. Yu. Ivanov, V. D. Travkin, A. M. Balbashov, and A. Loidl, Nat. Phys. **2**, 97 (2006).
[9] H. Katsura, A. V. Balatsky, and N. Nagaosa, Phys. Rev. Lett. **98**, 027203 (2007).
[10] Y. Takahashi, R. Shimano, Y. Kaneko, H. Murakawa, and Y. Tokura, Nat. Phys. **8**, 121 (2012).
[11] R. Valdés Aguilar, M. Mostovoy, A. B. Sushkov, C. L. Zhang, Y. J. Choi, S-W. Cheong, and H. D. Drew, Phys. Rev. Lett. **102**, 047203 (2009).
[12] J. S. Lee, N. Kida, S. Miyahara, Y. Takahashi, Y. Yamasaki, R. Shimano, N. Furukawa, and Y. Tokura, Phys. Rev. B **79**, 180403(R) (2009).
[13] M. Mochizuki, N. Furukawa, and N. Nagaosa, Phys. Rev. Lett. **104**, 177206 (2010).
[14] S. Miyahara and N. Furukawa, J. Phys. Soc. Jpn. **81**, 023712 (2012).
[15] T. Arima, J. Phys. Condens. Matter **20**, 434211 (2008).
[16] L. D. Barron, *Molecular Light Scattering and Optical Activity* (Cambridge University Press, Cambridge, England, 2004).
[17] T. Goto, Y. Yamasaki, H. Watanabe, T. Kimura, and Y. Tokura, Phys. Rev. B **72**, 220403(R) (2005).
[18] During the optical measurement, no dc electric field was applied to the sample. Formation of the single ferroelectric domain was confirmed by the pyroelectric current after the optical measurement.
[19] R. M. Hornreich and S. Shtrikman, Phys. Rev. **171**, 1065 (1968).
[20] In the ab-plane cycloidal spin state, the external magnetic field along the c axis renders $M \parallel c$ and $P \parallel a$. The light with ($E^{\omega} \parallel c$, $H^{\omega} \parallel a$) excites the SC-driven electromagnon, where the response from exchange-striction mode ($E^{\omega} \parallel a$) is absent.
[21] T. Roth and G. L. J. A. Rikken, Phys. Rev. Lett. **88**, 063001 (2002).
[22] G. L. J. A. Rikken, C. Strohm, and P. Wyder, Phys. Rev. Lett. **89**, 133005 (2002).
[23] M. Kubota, T. Arima, Y. Kaneko, J. P. He, X. Z. Yu, and Y. Tokura, Phys. Rev. Lett. **92**, 137401 (2004).
[24] J. H. Jung, M. Matsubara, T. Arima, J. P. He, Y. Kaneko, and Y. Tokura, Phys. Rev. Lett. **93**, 037403 (2004).
[25] M. Saito, K. Taniguchi, and T. Arima, J. Phys. Soc. Jpn. **77**, 013705 (2008).
[26] I. Kézsmárki, N. Kida, H. Murakawa, S. Bordács, Y. Onose, and Y. Tokura, Phys. Rev. Lett. **106**, 057403 (2011).
[27] K. Marinov, A. D. Boardman, V. A. Fedotov, and N. Zheludev, New J. Phys. **9**, 324 (2007).
[28] M. Mochizuki and N. Nagaosa, Phys. Rev. Lett. **105**, 147202 (2010).